DOE/ET/20279-215

Distribution Category UC 63a-e

PHOTOVOLTAIC I-V CURVE MEASUREMENT TECHNIQUES

DOE/ET/20279--215

DE83 000447

August 1982

C.H. Cox

T.H. Warner*

Electric Power Systems Engineering Laboratory

Massachusetts Institute of Technology

Massachusetts Institute of Technology

Lincoln Laboratory

Lexington, Massachusetts 02173-0073

Prepared for

THE U.S. DEPARTMENT OF ENERGY

UNDER CONTRACT NO. DE-AC02-76ET20279

Blank Page

ABSTRACT

Performance evaluation of photovoltaic (PV) arrays under actual field conditions provides important feedback to the module design process. One of the principal methods for assessing an array's performance is to plot its current, I, versus voltage, V, curve. Following a brief review of techniques for measuring the I-V curve, a new, capacitive-based approach is presented. It uses a rapid sweep of the I-V curve that substantially reduces the average power transfer between array and load, and in turn, substantially reduces the size and weight of the curve tracer. Both theoretical and practical aspects of the approach are presented for a 10-kW unit. Performance is verified by comparison with I-V curves obtained by using a conventional load. The agreement is found to be excellent. Approximately an order of magnitude reduction in size, weight and power consumption over conventional units was realized with the experimental I-V curve tracer.

Blank Page

TABLE OF CONTENTS

LIST OF FIGURES

List of Figures (con'd)

1.0 INTRODUCTION

Performance evaluation of photovoltaic (PV) arrays under actual field conditions provides important feedback to the module design process. The two principal tools used for assessing array performance are the infrared (IR) camera and the current-versus-voltage (I-V) curve tracer.

The IR camera has been applied in two different ways. One use is as an inspection device for locating cracks in cells within modules (1). Since silicon is transparent to radiation wavele longer than its band gap (about 1.1 μm), illuminating the module with, for example, 1.2 μm light enables an IR camera to view the light scattered off cracks in the PV cell--even those on its back surface. The second application of IR cameras is based on the fact that defective portions of the array do not produce the same electrical output as functional portions, thus temperatures of defective portions differ from those of the normally operating portions that surround them. Viewing a sunlit array, an IR camera can be used to find those portions of the array that are operating at a different, usually higher, temperature (2). Although somewhat cumbersome as presently implemented, the fundamental limitation of the IR camera is that it can only find a problem that results in a measurable temperature difference; it is incapable of finding minor temperature changes caused, for example, by open circuits, or of assessing the performance of a fully operating array.

The second principal tool for assessing array performance is the I-V curve tracer; i.e., a device that measures and plots the current, I, versus voltage, V, curve of the array. As can be seen from Fig. 1, the I-V curve has characteristic shapes for normally operating arrays, shown by the dashed lines in all three parts of the figure, as well as for all the major array failure modes, shown by the solid lines.* Thus the curve tracer is capable of assessing normal and abnormal arrays. In fact, it is not always necessary to measure the entire I-V curve. Hence the discussion begins with a review of I-V curve measurement techniques and their applications. When the entire I-V curve is required, a swept technique is described that offers substantial savings in size and weight over conventional I-V curve measurement approaches. Details of the theory and practice of the swept approach are presented.

---

*The inverse function, i.e., identifying the failure mode based on the I-V curve, is not always unique. In some instances, more than one failure mode can have the same I-V curve.

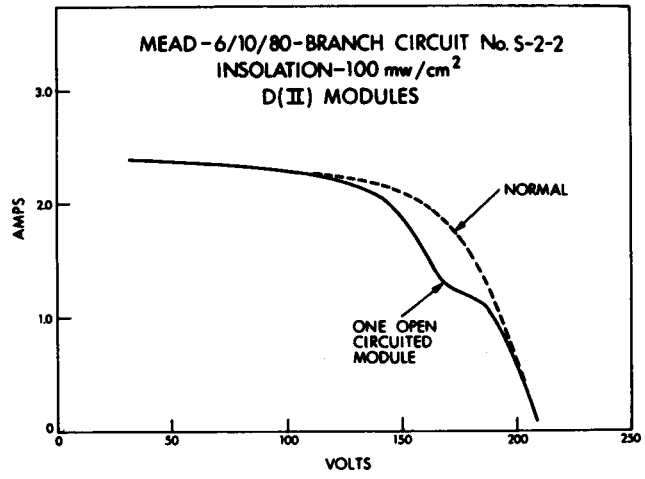

C74-1229

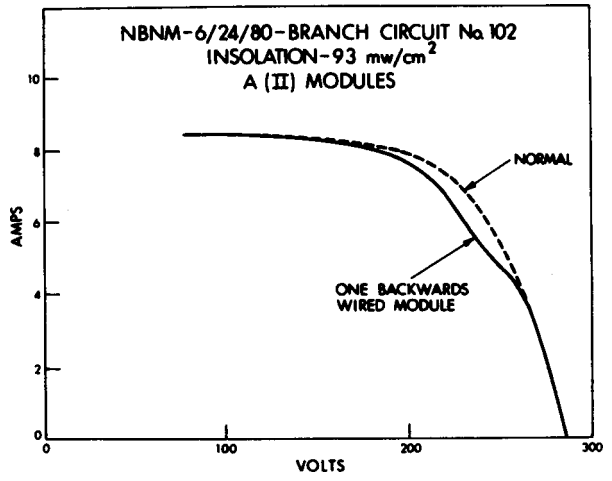

C74-1228

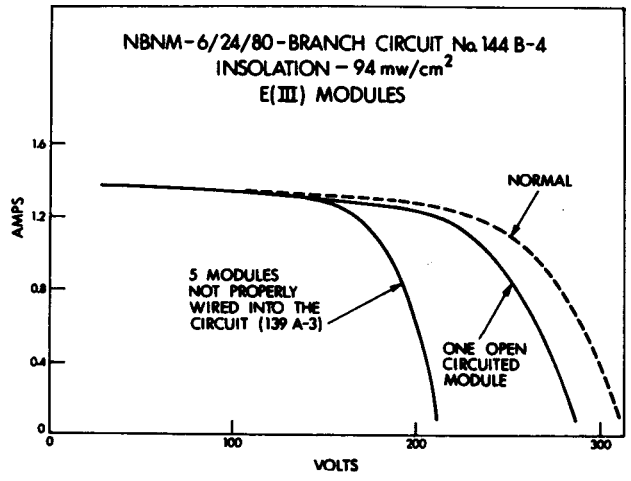

C74-1227

Figure 1. Representative I-V curves from normal arrays (dashed lines) and under various degradation modes: (top) open-circuit module with a bypass diode; (middle) one module wired with reverse polarity; and (bottom) open-circuited module without bypass diode.

2.0 REVIEW

The standard, lumped, low-frequency equivalent circuit for a PV cell is shown in Fig. 2a. Independent of the conditions at its terminals, the cell contains an ideal current source whose output magnitude is dependent on insolation. Loss mechanisms within the cell and its contacts are represented by two resistances, series and shunt, together with a silicon diode. The corresponding current-versus-voltage and power-versus-voltage curves are shown in Figs. 2b and 2c, respectively. With no voltage across the cell, i.e., the cell operating into a short circuit, all the current from the source flows through the external circuit. For voltages across the cell that are low compared to a silicon diode's forward drop, the cell continues to appear as an ideal current source, degraded by the resistance terms.

As the voltage increases, the diode begins to divert increasing amounts of the current, until eventually all the current is diverted internally. Also shown in this figure are all the principal points on an I-V curve: I_{sc}, V_{oc}, I_{mp} and V_{mp}.

As previously mentioned, it is not always necessary to measure the entire I-V curve. For example, measurement of I_{sc} and V_{oc} gives a simple alive or dead indication. Such measurements can be made with most hand-held multimeters, at least at the module level. Since a PV device is current limited, both I_{sc} and V_{oc} can be measured by simply connecting the multimeter directly across the module. This type of test is often useful just prior to module installation.

Should points in between I_{sc} and V_{oc} be required, a variable resistor can be employed. At low powers, such as those obtainable from individual modules, a rheostat can be used. For higher powers, typical of strings of modules, a combination of switches and individual power resistors is more feasible than a rheostat. This latter approach has been implemented, using 32 resistors, for measuring strings of modules as discussed in Reference 3. Extending this approach to achieve greater resolution rapidly becomes feasible.

Not all points on the I-V curve are equally interesting. If, for example, one needs to monitor the maximum power point, a programmable load can be used. At present, these loads are limited to 2500 W and cannot operate the array with less than 50 V across it. (They generally do have a switch for forcing short-circuit conditions.) The PV system's power conditioner might also be

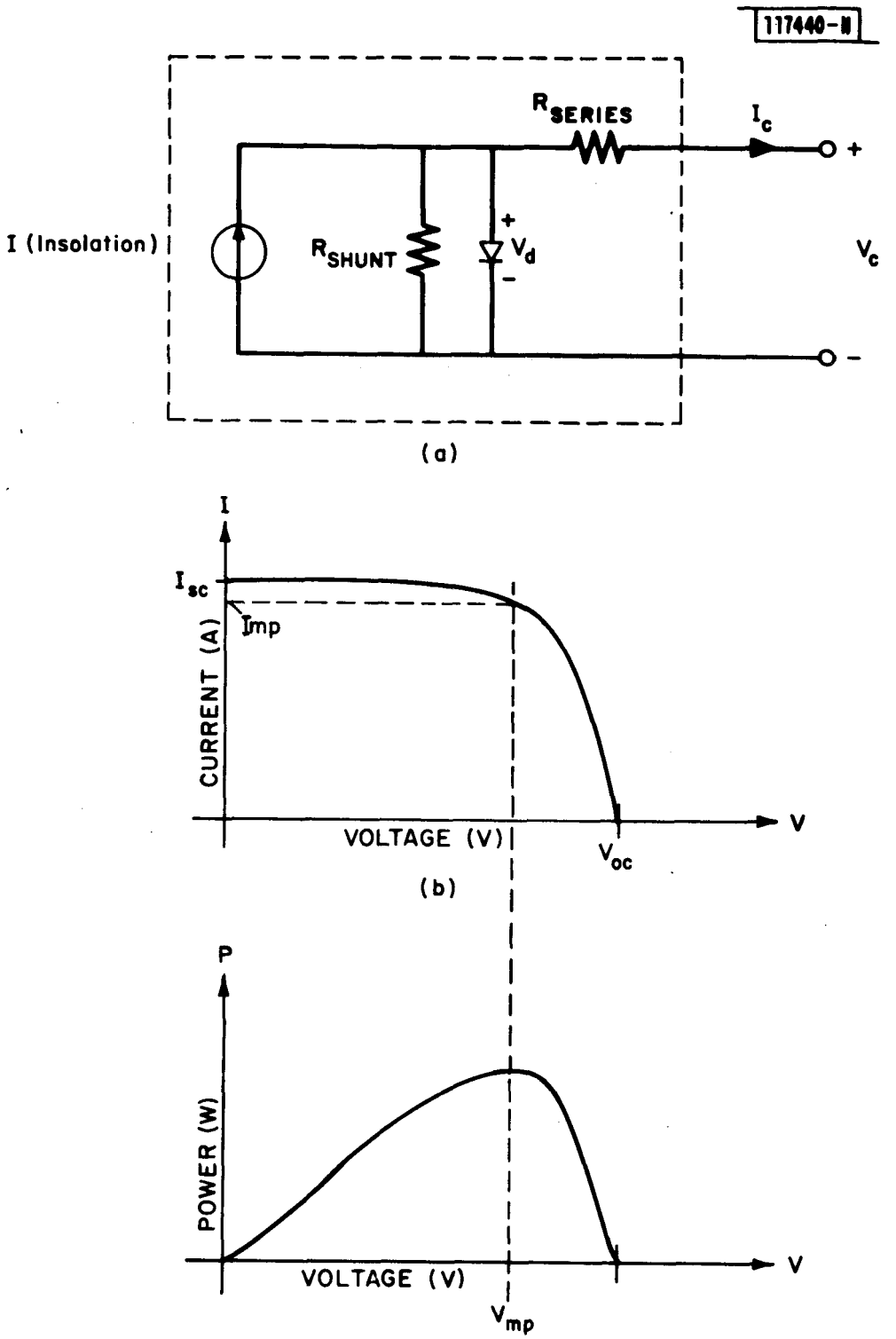

Figure 2. (a) Lumped, low-frequency equivalent circuit of a solar cell and plots of its current-versus-voltage (b) and power-versus-voltage (C) characteristics.

used to track the maximum power point--provided it has a good tracking algorithm. Further, since power-conditioner efficiency is generally a function of power level, power measurements must be made at the input of the unit.

Recent work (4) indicates that there is only a 1-4% annual energy advantage to tracking the maximum power point over operating at a constant voltage, even under a wide range of array degradation conditions. Thus to replicate this type of array operation, a power zener diode can be used, though power zeners are available only up to about 100 W.

If good resolution of the I-V curve is required at moderate power levels, i.e., up to 10 kW, the swept approach presented below can be appropriate. The sweeping approach trades the ability to monitor one point in the I-V plane continuously for the portability that is often useful in the field. By making a relatively rapid sweep of the I-V curve, the average power dissipation of the curve tracer is substantially reduced, thereby permitting size and weight reduction of the curve tracer.

A particularly convenient way to implement a sweeping-type curve tracer is to use a capacitor as the main load. The basis concept (5) is quite simple, as shown in Fig. 3. Initially, the switch is closed, the capacitor is discharged, and the array is operating at short circuit. When the switch is opened, the initial voltage across the capacitor cannot change instantaneously, since the array current is finite. The array current flows into the capacitor and charges it according to the familiar capacitor equations:

$$V_C(t) = \frac{1}{C}\int_0^t i(\tau)\, d\tau. \qquad (1)$$

As the charging progresses, a data-acquisition system measures the voltage and current of the array and plots them parametrically.

C74-1262

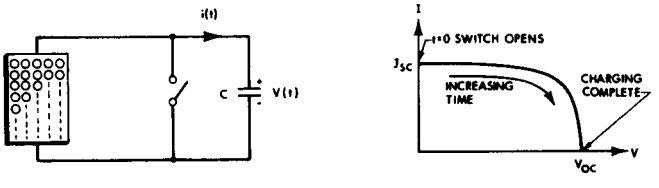

Figure 3. Use of a capacitor to measure the I-V curve: basic capacitor-charging topology, left, and resultant I-V curve.

3.0 SWEEPING - THEORY

The I-V curve provides a basic description of the dc performance of a wide variety of electronic components. Practical interest centers on components whose I-V curve is expressable as a single valued function of either voltage or current; i.e., a given value of voltage must result in a unique current or vice versa. For example, the I-V functions of four common components, a resistor, R; a diode, D; a current source, C; and a voltage source, V; are as follows:

$$I_R(V_R) = \frac{V_R}{R} \tag{2}$$

$$I_D(V_D) = I_S(e^{\frac{qV_d}{kT}} - 1) \tag{3}$$

$$I_C(V_C) = I_o \tag{4}$$

$$V_V(I_V) = V_o \tag{5}$$

The I-V curve for any of these devices is readily determined by fixing the current and calculating the resulting voltage. In the case of a resistor, for example, a fixed value of current results in a single voltage level. Taken together, the I and resulting V values can be plotted as a point in the I-V plane, as shown in Fig. 4a. A succession of values of I results in a succession of voltage levels. The resulting I-V curve is a line in the I-V plane. When two components are interconnected, the operation of the combination is the value of current and voltage that simultaneously satisfies the I-V functions of the interconnected components. In graphical terms, the operation of the combination can be found by plotting both I-V curves on the same axes and finding their intersection. Except for degenerate cases, this intersection will be a point*.

The conventional approach to measuring the I-V curve of a given component begins by connecting it to another "load" component. The load component's

*In some cases, such as with a resistor and a tunnel diode, the intersection could be a set of three points. Not all of these points, however, represent stable operation. Hence, after a finite time the combination will be operating at one of the intersection points.

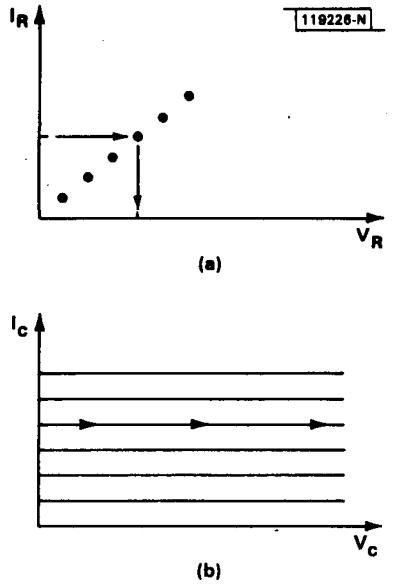

Figure 4. (a) Construction of the I-V curve of a resistor from a succession of points determined by various current values and (b) construction of the I-V region of a capacitor from a succession of lines determined by various current values.

I-V curve is then varied; e.g., if the load is a resistor, its value is changed, and the succession of intersection points in the I-V plane so generated produces the I-V curve of the given component.

To analyze the sweeping technique introduced above, it is necessary to determine the I-V curve of a capacitor. Its I-V function is:

$$I_C(V_C) = \frac{CdV_C}{dt}. \tag{6}$$

Notice that there is a fundamental difference between a capacitor's I-V function and those given above for a resistor, diode, etc. The capacitor I-V function depends upon time; specifying I and V for a capacitor does not uniquely specify a point in the I-V plane. In fact, a fixed I or V can generate a multiplicity of points. For example, suppose, as was done to determine the resistor's I-V curve above, that $I_C = K_C$; i.e., a constant independent of time. Then $V_C = kt$, i.e., a ramp function. Thus a constant current input driving a capacitor generates a series of voltages whose magnitude increases linearly with time. Graphically this plots as a horizontal straight line, as

shown in Fig. 4b. Different magnitudes of current displace the horizontal line vertically. Therefore the I-V "curve" of a capacitor is not a one-dimensional line but a two-dimensional region of the I-V plane.*

In using a capacitor to measure the I-V curve of a given component, the resulting operation of the combination is still the intersection of the two individual I-V curves. If the given component's I-V curve is a line, then the intersection with the capacitor's region will be the I-V line of the given component.

To be effective, the capacitor's I-V region must at least contain the portion of the I-V plane in which it is desired to measure the I-V curve. In order to explore the allowable regions, the conventions for voltage and current polarity shown in Fig. 5a will be adopted. The capacitor's allowable regions are shown by the shaded areas in Fig. 5b. If the initial charge on the capacitors is zero; i.e., $V_C\ (t = 0) = 0$, then the allowable regions are all of quadrants I and III, but none of quadrants II and IV are accessible. In order to measure I-V curves in these quadrants, an initial charge must be placed on the capacitor. As shown in Fig. 5b, an increasing positive initial charge increases the coverage in quadrant IV at the expense of quadrant I coverage while leaving quadrants II and III unaffected. Similarly, an increasingly negative initial charge expands coverage into quadrant II, sacrifices coverage in quadrant III, and leaves quadrant I and IV unaffected.

Thus measurement via one continuous sweep of the I-V curve of devices within any one quadrant is possible provided the necessary initial capacitor voltage can be applied. Further, continuous sweeping of the I-V curve through two quadrants is possible for the quadrant pairs (I, II) and (III, IV), depending upon the magnitude and polarity of the precharge. No initial conditions can permit continuous sweeping between the remaining adjacent quadrant pairs, at least for a capacitor.

By expanding consideration to inductive loads, one obtains results that are, in some sense, complementary to those obtained for capacitor loads. Again, the I-V "curve" for an inductor is a region of the I-V plane. The

---

*If another time function is chosen for I, then it is still possible to cover the I-V plane, but lines are not simply horizontal. For example, if $I_C = kT$; i.e., a ramp function, then the I-V plane is covered with parabolic lines.

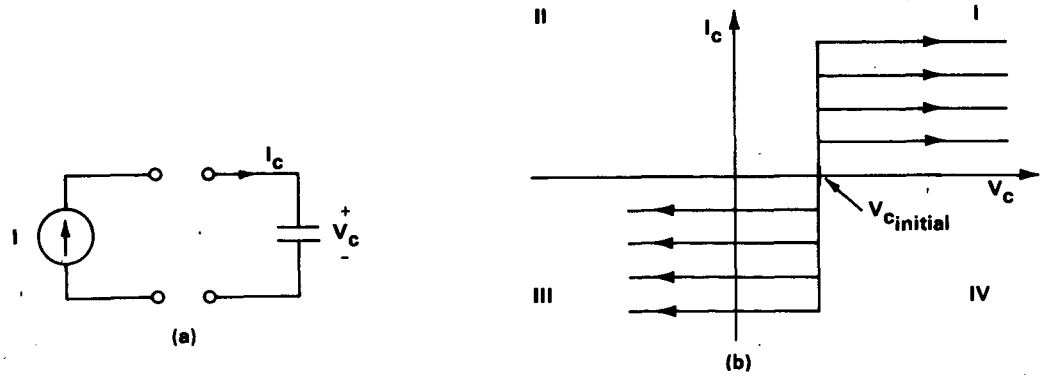

Figure 5. (a) Voltage and current conventions used to specify the portions of the I-V plane covered by a capacitor, (b) with an initial charge as shown.

regions covered by an inductor with connection as defined in Fig. 6a are shown in Fig. 6b. Notice that the adjacent quadrant pairs where continous sweeping can and cannot be done are the exact complement to the capacitor case. Therefore, by choosing the appropriate element--capacitor or inductor--and the appropriate initial conditions, continous sweeping coverage of any single or adacent quadrant pair is possible.

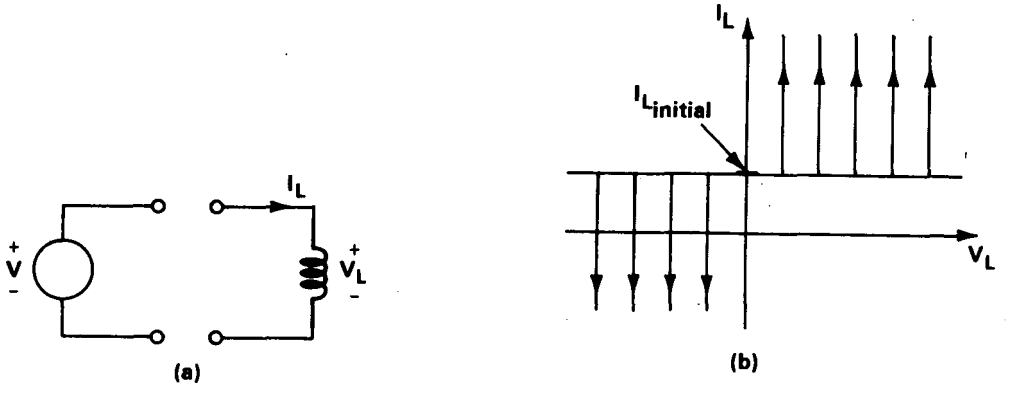

Figure 6. (a) Voltage and current conventions used to specify the portions of the IV plane covered by an inductor, (b) with an initial current as shown.

4.0 SWEEPING - IMPLEMENTATION

This measurement method hinges on finding a suitable capacitor. Clearly it must be rated to handle V_{oc} and I_{sc}, at least on a surge basis. As shown below, array power is not the best parameter for determining the value of capacitance required. To see this, assume the array has a fill factor of one. Equation (1) can then be solved easily. The capacitor voltage simply ramps up from zero to the open-circuit voltage, V_{oc}, in a time, T_{scan}. When the array reaches V_{oc}, the current drops to zero and the charging stops:

$$V_{oc} = \frac{I_{sc}}{C} T_{scan}. \tag{7}$$

This equation can be rearranged to find the capacitor size necessary to produce a predetermined scan time:

$$C = \frac{I_{SC}}{V_{oc}} T_{scan}. \tag{8}$$

Equation (8) shows that the ratio of short-circuit current to open-circuit voltage is the key parameter for determining the value of capacitance required. A minimum scan time should be chosen such that the swept I-V curve very closely approximates the I-V curve obtained using steady-state methods. The Large Area Pulsed Solar Simulator* (LAPSS) obtains good results with a scan time of two milliseconds. If a 2000 μF capacitor is chosen, the curve tracer will be able to handle any module or array with:

$$\frac{I_{sc}}{V_{oc}} \leq 1. \tag{9}$$

This includes all residential arrays and new low-voltage, high-current model designs. Capacitors in the 1000-μF, 450-V range are available from many manufacturers and are about the size of a 12-ounce soft drink can.

To help visualize the tradeoffs between array power-handling capability, capacitance value and scan time, Fig. 7 has been prepared. The assumption of a fill factor of one has again been used. Contours of constant T_{scan}, in seconds, are shown by the radial, solid lines. The dotted hyperbolas indicate countours of constant array power, P_a, where $P_a = I_{sc}V_{oc}$. It can be seen,

---

*Manufactured by Spectrolab, Inc.

for example, that rapid (respectively slow) scan times are more closely associated with high I_{sc} (respectively V_{oc}) than high (respectively low) power levels.

C74-1263

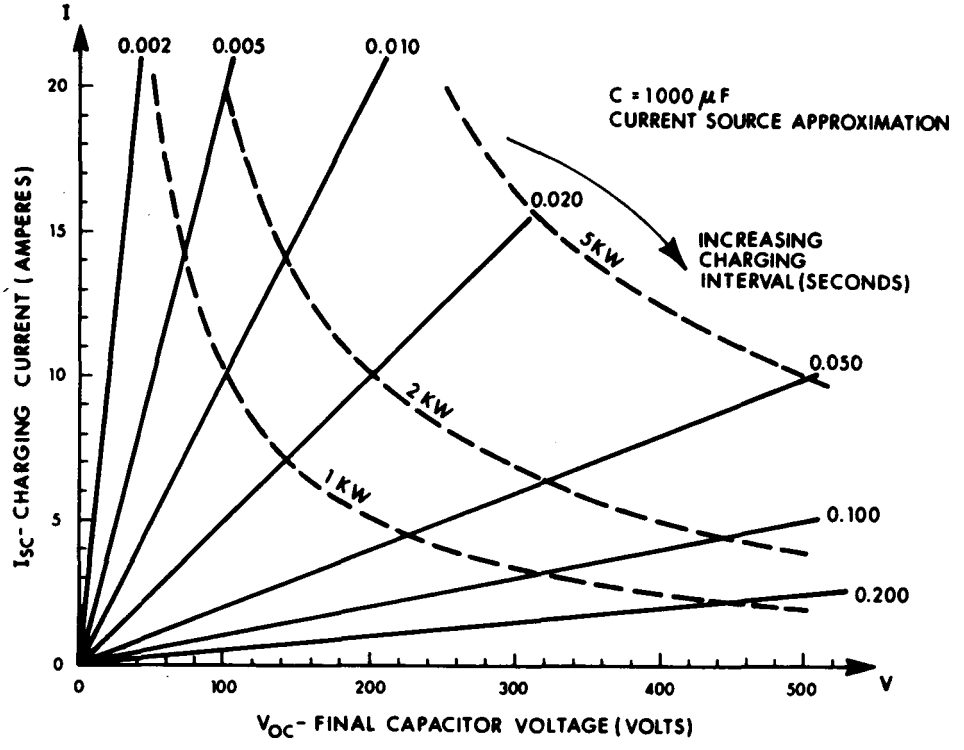

Figure 7. Isobars in the I-V plane of constant charging interval, T_{scan}, shown by the solid, radial lines and of constant power, shown by the dotted hyperbolas.

The reduction in size and weight of the swept approach, when compared to conventional steady-state approaches, is principally a result of the reduction in average power dissipation. A steady-state unit must be capable of dissipating, continuously, the power at any point along the I-V curve. The maximum-power dissipation will occur at the maximum power point, which for the fill factor of 1 array occurs at V_{oc}:

$$P_{avg.\ ss} = I_{sc}V_{oc}. \tag{10}$$

For the swept approach, the average power dissipation is the energy stored on the capacitor times the frequency of measurements:

$$P_{avg,\ sw} = 1/2\ CV_{oc}^2 f_m \tag{11}$$

where $F_m = \frac{1}{T_{sts}}$ and T_{sts} is the time between the initiation of two sequential scans. Since it is usually the case that $T_{sts} \gg T_{scan}$, the average array power dissipation for the swept approach can be quite low. Also notice that, unlike the steady-state average power dissipation, the swept average power dissipation is independent of I_{sc}.

As an example, suppose one has a 5-kW array where I_{sc} = 20 A and V_{oc} = 250 V. Continue to assume FF = 1. For the steady-state load:

$$P_{avg,\ ss} = 5000\ W.$$

To calculate $P_{avg,sw}$, C, T and T_{sts} must be chosen. For C = 1000 μF, equation (7) yields:

$$T_{scan} = 12.5\ msec.$$

If $T_{sts} = T_{scan}$; i.e., if the capacitor is discharged immediately and instantly so that another sweep can begin, the average dissipation of the swept approach is:

$$P_{avg,\ sw} = 2500\ W.$$

This represents a reduction in average power dissipation of only a factor of 2 over the steady-state approach. As a more realistic lower bound on the time between measurements, assume T_{sts} = 5 sec. For this case:

$$P_{avg,\ sw} = 6.25\ W.$$

The reduction in average power handling capability is:

$$\frac{5000}{6.25} = 800.$$

Although the reduction in power is substantial, it is not totally translated into a reduction in size because a significant amount of electronics is required to record the I-V curve as it is being swept.

In order to determine the degree of reduction that is feasible and to address some of the implementation issues, an experimental unit was constructed. It consists of two units, shown in Fig. 8a: a data-acquisition unit (DAU) and a an HP-85. The DAU, a close-up of which is shown in Fig. 8b, contains all of

the power electronics, data acquisition, short-term memory, and control electronics to run the measurement. The data display, storage and analysis is provided by an HP-85 desk-top computer. The DAU and HP-85 communicate via an IEEE-488 instrumentation bus.

CP267-6400

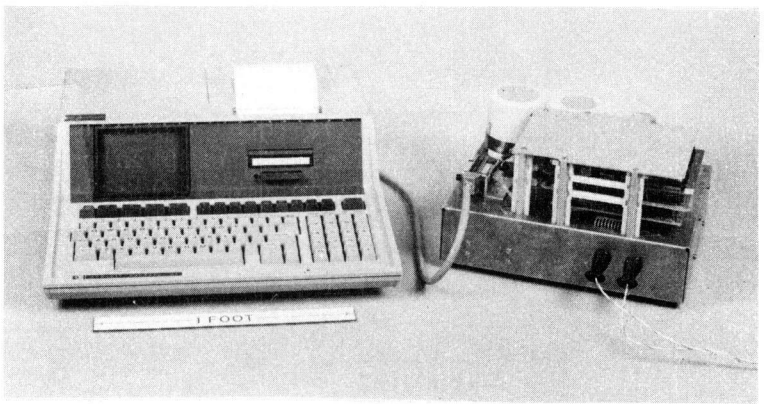

CP267-6204

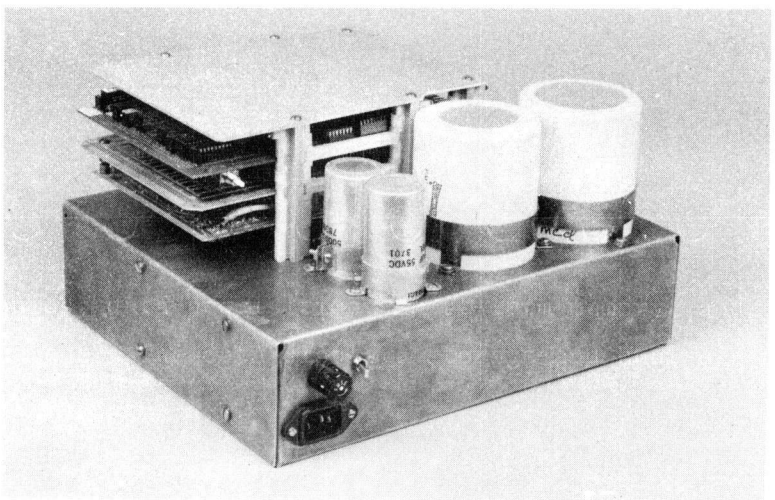

Figure 8. Photograph (top) of 10-kW capacitive curve tracer showing data acquisition unit (DAU), right, and HP-85; (bottom) close-up view of DAU.

A block diagram of the system is shown in Fig. 9. Initially, switch 1 is closed, 2 and 3 are open. This allows the capacitor to be charged to a negative voltage. When switch 1 is opened and 2 is closed, a negative voltage will be placed across the array. The I-V curve will actually start in the reverse-bias region, proceed through short circuit and continue all the way to open circuit. In this manner the entire forward operating characteristic can be plotted. Once the curve is complete, switch 2 is opened and 3 is closed to discharge the capacitor for the next measurement.

C74-1261A

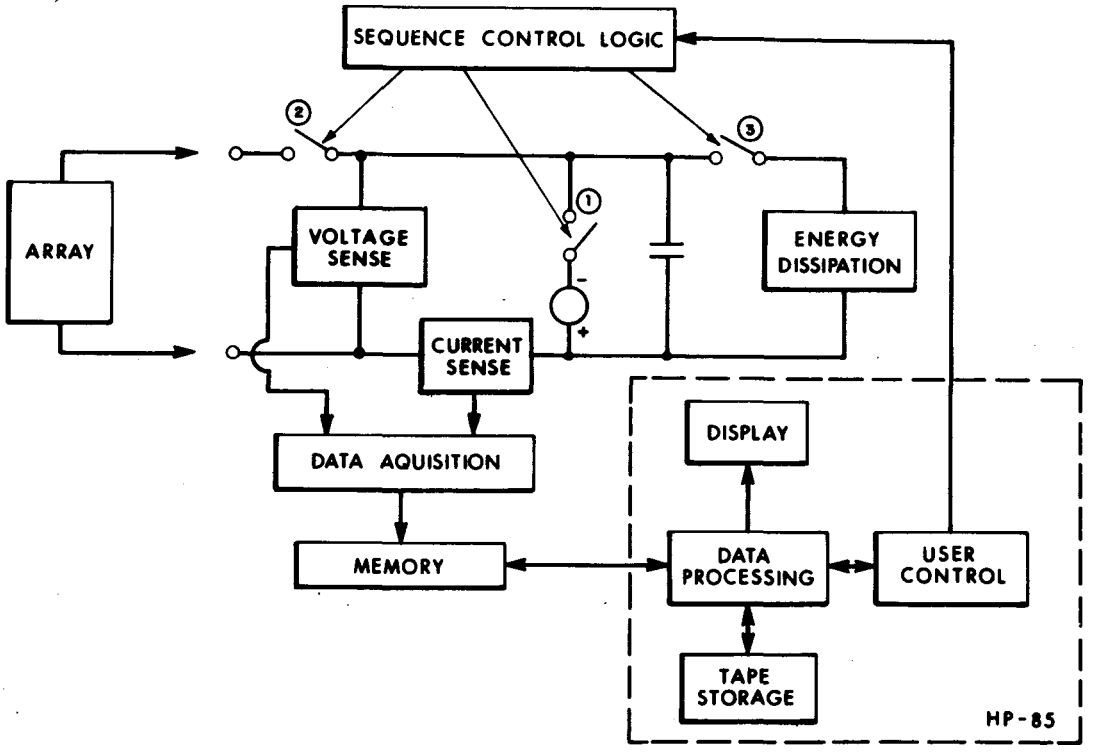

Figure 9. Block diagram of the curve tracer showing functions implemented in the DAU and in the HP-85 surrounded by dotted line.

During the capacitor charge-up, the DAU samples and quantizes the voltage and current. The overall accuracy desired was $\pm 1\%$. In turn this requires at least 7 bits of quantization. To allow more flexibility in the apportionment of the error budget, 8-bit A/Ds were used. The maximum A/D conversion rate required depends upon the minimum T_{scan} which in turn depends

upon the size of the capacitor. From the discussion presented earlier, a reasonable minimum value of T_{scan} is 10 msec. With 256 samples (8 bits) required within the minimum T_{scan}, the resulting total conversion time per sample--including sample and hold, A/D conversion and memory store--is about 40 μsec. This is well within the capabilities of available, high-speed data conversion products.

The data rate corresponding to 40 μsec conversion is 25 kbytes/sec. The IEEE-488 bus will easily handle such a data rate; unfortunately, the HP-85 I/O will not. Thus the digitized I-V curve will need to be stored in a memory within the DAU as it is acquired during T_{scan}. Upon completion of a sweep, the data can be transferred from the DAU to the HP-85 at a mutually convenient rate.

In order to run the complete measurement from the HP-85, the DAU must be capable of both TALK and LISTEN bus functions. With this capability, range setting can also be done from the HP-85. Ancillary functions, such as capacitor discharge and auto-zero of the DAU, are generated by the HP-85 software, thereby freeing the operator from attention to these details.

Of particular interest for the verification of the swept approach is the degree to which an I-V curve taken with this method matches an I-V curve taken with a conventional load such as a Dynaload*. A block diagram of the setup used to determine the match is shown in Fig. 10. The ramp generator insures a smooth continuous sweep by the Dynaload. By choosing a very slow sweep, e.g., 10 seconds, it is possible to avoid the potentially distorting effects introduced by dynamics in the array, Dynaload and X-Y plotter. Thus the I-V curve generated in this manner can serve as the reference curve. A switch is provided for alternatively connecting the new curve tracer to the same array. As it is impractical to place arrays with these power levels in a solar simulator, the test was conducted on an outdoor, ground-mounted array located at the Systems Test Facility (6). To minimize errors due to variation in insolation, the test was conducted around noon on a day with clear skies. The outputs from both methods were then plotted on the same graph.

*Manufactured by Transistor Devices, Inc.

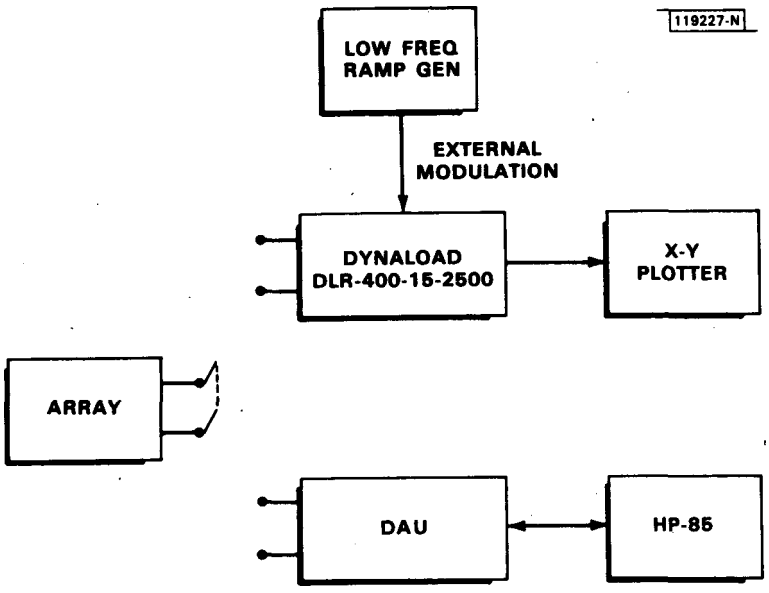

Figure 10. Block diagram of test setup for comparing the I-V curve obtained with the new capacitive tracer and the conventional load approach.

First, I-V curves were generated on a fully operational array. The results are shown in Fig. 11, with the reference curve indicated by the dotted line and the capacitive swept curve indicated by a solid line. Overall, agreement is quite good. The digitization of the swept curve is more noticeable than seems reasonable, and this contributes to the mismatch in current between the two curves over the interval 105 to 175 volts. Well after this curve was made, it was discovered that two of the data lines, the LSB and the next higher bit, were interchanged.

With this error corrected, another comparison test was run, but this time on an array in which a failure existed. The resulting I-V curve, with a "glitch" in it, is shown in Fig. 12. As before, the dotted curve was produced by the reference equipment and the solid curve by the capacitive swept equipment. With the wiring error corrected, the digitization noise was reduced, resulting in excellent agreement between the curves generated by the two approaches.

One of the reasons for undertaking this work was to permit I-V curves to be made on arrays of higher power. Dynaloads are presently limited to

C74-1292

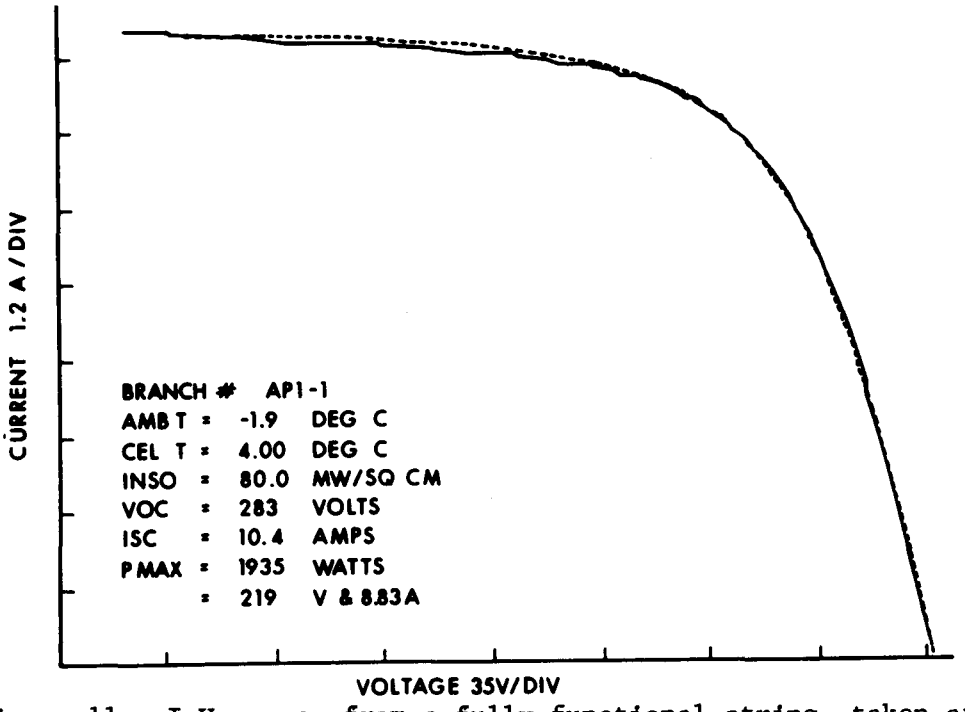

Figure 11. I-V curves from a fully functional string, taken at essentially the same time with the capacitive curve tracer (solid line) and the conventional load.

C74-1520

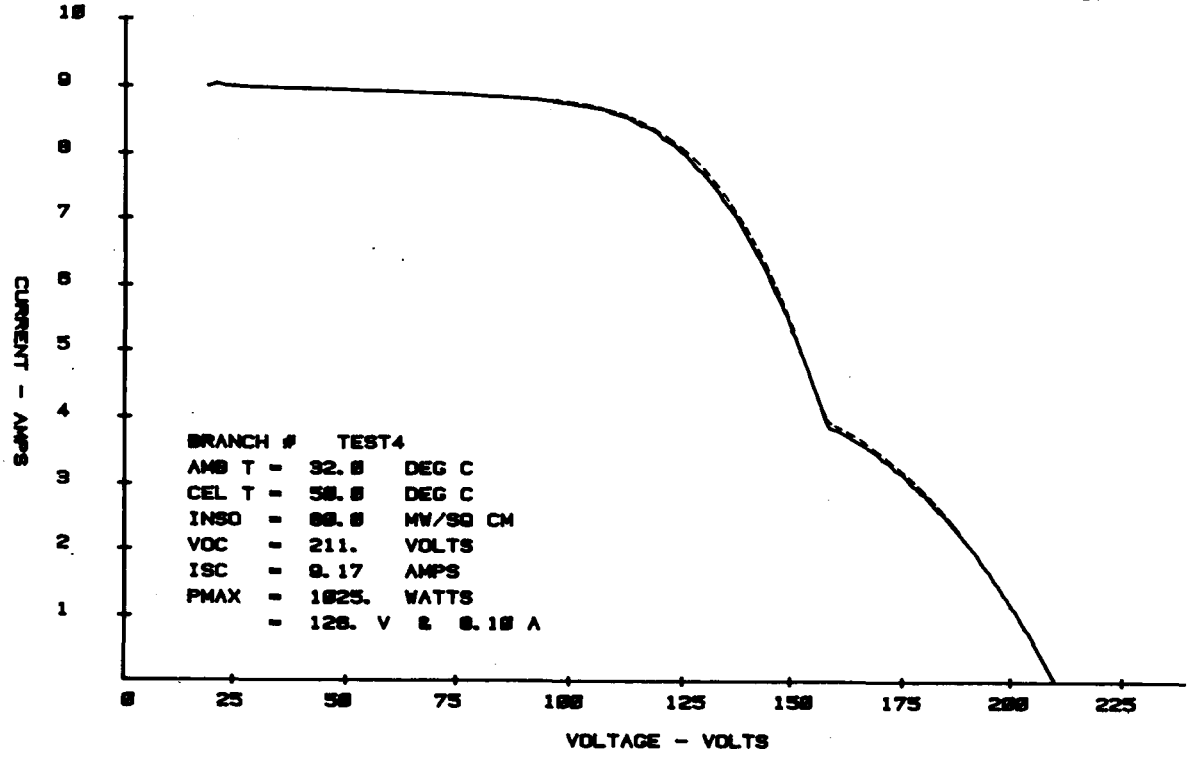

Figure 12. I-V curves from a degraded string, taken at essentially the same time with the capacitive curve tracer (solid line) and the conventional load.

about 2.5 kW. As designed, the capacitive curve tracer will handle up to 10 kW. An I-V curve of a 7.5 kWp array, operating near full power, is shown in Fig. 13.

C74-1628

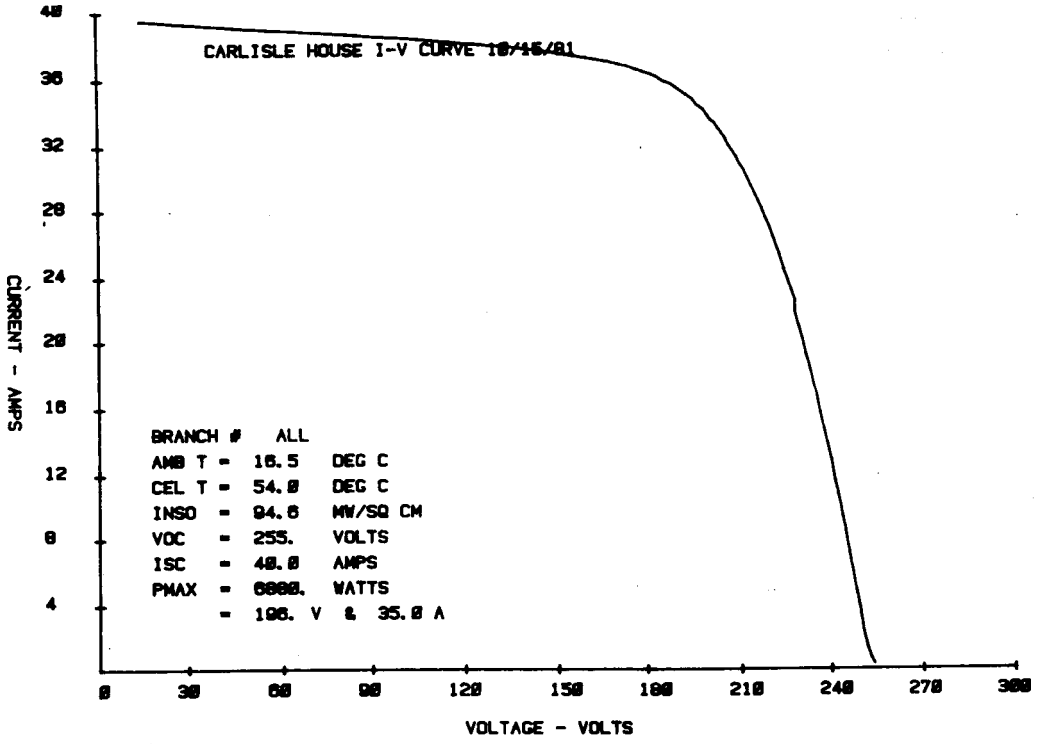

Figure 13. I-V curve of a 7.5-kWp array operating near full power with the capacitive load curve tracer.

A comparison of some of the principal parameters of a conventional and capacitive I-V curve tracer is shown in Table I for units capable of measuring 10-kW arrays. There is roughly an order of magnitude reduction in all three areas.

TABLE I

COMPARISON OF 10-kW I-V CURVE TRACERS

	Conventional	Capacitive
Weight (lbs)	125	13
Size (cu. ft.)	4.3	0.5
AC Power (W)	240	20

5.0 SUMMARY AND CONCLUSIONS

A variety of techniques are available for testing specific aspects of a PV array. Following a brief review of these, a new capacitive approach for measuring the entire I-V curve when such a complete measurement is required is presented. The approach uses a rapid sweep of the I-V curve, thereby reducing the average power-handling requirements of the curve tracer significantly. An experimental unit was constructed in order to verify the proposed technique. The unit is portable enough to be suitable for both laboratory and field use. Over the past year and a half, the new curve tracer has been used at numerous field test sites throughout the United States (7). Often the status of an array could be determined from simple inspection of the I-V curve, since many failures result in characteristic changes in the I-V curve shape (8).

The power-handling capability of the experimental curve tracer was chosen to cover the power output of PV systems targeted for residential use--all of which are less than 10 kWp. Extension of the capacitive concept to other power levels certainly appears feasible; the question is--is it desirable. At lower power levels, the overhead in terms of the electronics necessary to sample the curve becomes the dominating size factor. This, together with the fact that other techniques are feasible at these levels, would reduce the desirability of building a capacitive unit for lower powers. Conversely, at higher powers the desirability increases. A 100-kWp curve tracer, for example, would need 20,000 to 40,000 μF of capacitance; yet this would only double the size of the present curve tracer. All the other high power elements should be readily available. The desirability of using a capacitive approach for high power levels is enhanced by the fact that achieving I-V measurement capabilities at such power levels would be exceedingly difficult by conventional means.

ACKNOWLEDGMENTS

The authors would like to thank members of the Energy Systems Engineering staff, particularly S. E. Forman and E. E. Landsman, for many helpful discussions. Further appreciation is extended to Joe Chludzinski and Mike Wong for assistance in constructing the prototype and to Sharon Howland for typing the manuscript.

REFERENCES

1. Forman, S. E. and Caunt, J. W., "A Portable, X-Y Translating Infrared Microscope for Remote Inspection of Photovoltaic Solar Arrays," International Symposium for Testing and Failure Analysis, Los Angeles, CA, 27 October 1980, (Also MIT Lincoln Laboratory Technical Report No. DOE/ET/20279-101).

2. Glazer, S. D., "Hot-Spot Heating Studies," Proceedings of the 18th Project Integration Meeting, Low-Cost Solar Array Project, JPL, Pasadena, CA, February 1981, DOE/JPL-1012-58.

3. Solman, F. J., et al., "Maintenance Manual for the PV Power System at Natural Bridges National Monument," MIT Lincoln Laboratory Technical Report No. DOE/ET/20279-177 (to be published).

4. Branz, H. M., Hart, G. W. and Cox, C. H., III, "The Photovoltaic Array/Inverter Interface," MIT Lincoln Laboratory Technical Report No. DOE/ET/20279-170 (to be published).

5. Cull, R. C. and Forrestieri, A. F., "The DOE/LeRC Photovoltaic Systems Test Facility," IEEE Photovoltaic Specialists' Conference, 1978, pp. 22-26.

6. Sacco, S. B., "Facility Description for the MIT Lincoln Laboratory PV Test Facility," MIT Lincoln Laboratory Report No. C00-4094-41, June 1979.

7. Forman, S. E., "Performance of Terrestrial Photovoltaic Modules at MIT Lincoln Laboratory Experimental Photovoltaic Systems," MIT Lincoln Laboratory Technical Report No. DOE/ET/20279-140, April 1981.

8. Forman, S. E., "Usng Measurements to Detect Electrical Problems in Operational Photovoltaic Arrays," SERI Commercial Photovoltaics Measurement Workshop, Vail, CO, 27-29 July 1981 (also MIT Lincoln Laboratory Technical Report No. DOE/ET/20279-149).